Inorganic Chemistry

Article

pubs.acs.org/IC

Oxygen-Atom Transfer from Iodosylarene Adducts of a Manganese(IV) Salen Complex: Effect of Arenes and Anions on I(III) of the Coordinated Iodosylarene

Chunlan Wang,[‖,†] Takuya Kurahashi,[†,‖] Kensuke Inomata,[§] Masahiko Hada,[§] and Hiroshi Fujii*[,†,‖]

[†]Institute for Molecular Science and Okazaki Institute for Integrative Bioscience, National Institutes of Natural Sciences, Myodaiji, Okazaki 444-8787, Japan

[‖]Department of Functional Molecular Science, The Graduate University for Advanced Studies (SOKENDAI), Myodaiji, Okazaki 444-8787, Japan

[§]Department of Chemistry, Graduate School of Science, Tokyo Metropolitan University, 1-1 minami-Osawa, Hachioji, Tokyo 192-0397, Japan

Supporting Information

ABSTRACT: This paper reports preparation, characterization, and reactivity of iodosylarene adducts of a manganese(IV) salen complex. In order to systematically investigate steric and electronic factors that control reactivity and selectivity, we prepared iodosylarene adducts from iodosylbenzene, iodosylmesitylene, 2,4,6-triethyliodosylbenzene, and pentafluoroiodosylbenzene. We also investigated the effect of anions on I(III) by using chloride, benzoate, and *p*-toluenesulfonate. Spectroscopic studies using ^{1}H NMR, electron paramagnetic resonance, infrared spectroscopy, and electrospray ionization mass spectrometry show that these iodosylarene adducts are manganese(IV) complexes bearing two iodosylarenes as external axial ligands. Reactions with thioanisole under the pseudo-first-order conditions show that the electron-withdrawing pentafluorophenyl group and the *p*-toluenesulfonate anion on I(III) significantly accelerate the oxygen-atom transfer. The high reactivity is correlated with a weakened I−OMn bond, as indicated by IR spectroscopy and mass spectrometry. Stoichiometric reactions with styrenes show that both enantioselectivity and diastereoselectivity are dependent on the arenes and anions on I(III) of the coordinate iodosylarenes. Notably, the pentafluorophenyl group and the *p*-toluenesulfonate anion suppress the cis-to-trans isomerization in the epoxidation of *cis*-*β*-methylstyrene. The present results show that iodosylarene adducts of manganese(IV) salen complexes are indeed active oxygen-atom-transfer reagents and that their reactivity and selectivity are regulated by steric and electronic properties of the arenes and anions on I(III) of the coordinated iodosylarenes.

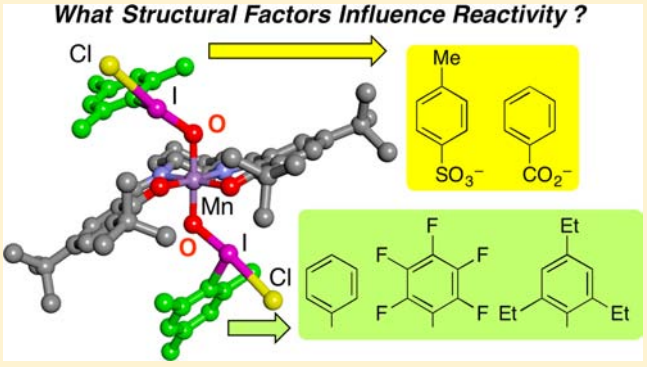

INTRODUCTION

Mechanistic aspects of oxygenation catalysis by transition metal complexes are of fundamental importance from the increasing demand for more efficient catalysts.[1] Oxygenation reactions are carried out in the presence of a small amount of a catalyst using a stoichiometric amount of a terminal oxidant. Among terminal oxidants, iodosylarenes are widely utilized as useful oxidants.[2] According to the consensus mechanism, an oxidant, such as an iodosylarene, is bound to a metal center, generating an oxidant adduct in the first step. In the subsequent step, the oxidant adduct is converted to a high-valent metal−oxo complex.

Hill et al. reported iodosylbenzene adducts of a manganese porphyrin complex, which were characterized as a precursor to active high-valent manganese−oxo species.[3] Nam et al. have also shown that an oxoiron(IV) porphyrin *π*-cation radical is a sole active species in an equilibrium mixture containing iodosylarene adducts of an iron(III) porphyrin complex.[4] Very recently, Lei et al. reported a detailed kinetic study for catalytic reactions by manganese porphyrins with soluble iodosylarene, which clarifies the pathway to reactive manganese(V)−oxo species via the formation of iodosylarene adducts.[5] In contrast, iodosylarene adducts of metal complexes do show oxygenation reactivity without the formation of high-valent metal−oxo species, as first pointed by Valentine et al.[6] They proposed that the electrophilicity of the I(III) center that is enhanced upon the binding to metal is responsible for the oxygenation reactivity of iodosylarene adducts. Consistent with their proposal, protonated iodosylarene monomers bearing I(III)−OH carry out oxygenation reactions, such as sulfoxidation, without activation by metal, as reported by Ochiai et al.[7] Bryliakov et al. also reported that, in the asymmetric sulfide

Received: May 21, 2013
Published: August 2, 2013

   dx.doi.org/10.1021/ic401270j | *Inorg. Chem.* 2013, 52, 9557−9566

oxidation by iron(III) salen complexes, iodosylarene adducts participate in catalytic oxygenation as key reactive species.[8]

There are rather complicated catalytic systems, in which both iodosylarene adducts and high-valent metal−oxo species coexist. Most notably, Goldberg et al. reported that a manganese(III) corrolazine generates a manganese(V)−oxo species in catalytic oxygenation reactions, but the active oxygenating species is not the manganese(V)−oxo but the iodosylbenzene adduct of manganese(V)−oxo.[9] Iodosylarene adducts of other metal−oxo complexes have also been proposed as active species.[10] It was also shown that epoxidation reactions catalyzed by porphyrin and salen complexes using iodosylarenes as a terminal oxidant are carried out by multiple active species including high-valent metal−oxo species and iodosylarene adducts,[11−13] because iodosylarene substituents and counterions of porphyrin and salen catalysts affect diastereoselectivity and enantioselectivity.

Although iodosylarene adducts of metal complexes have been frequently mentioned as a key intermediate, it is still unclear exactly what structural factors influence their reactivity and selectivity. This is mainly because structural information was not available for iodosylarene adducts of metal complexes. Very recently, McKenzie et al. reported the X-ray crystal structure of a nonheme iron(III) iodosobenzene adduct.[14] At almost the same time, we also reported the X-ray crystal structure of the iodosylmesitylene adduct of a manganese(IV) salen complex,[15] where salen is a chiral *N*,*N*′-bis(3,5-di-*tert*-butylsalicylidene)-1,2-cyclohexanediamine, a well-known catalyst for enantioselective olefin epoxidation.[16,17] As shown in Figure 1, the anion

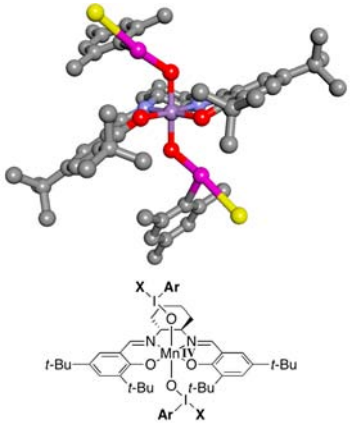

	Ar	X
Ph/Cl	C_6H_5	Cl
Mes/Cl	1,3,5-$(CH_3)_3$-C_6H_2	Cl
$Et_3C_6H_2$/Cl	1,3,5-$(C_2H_5)_3$-C_6H_2	Cl
C_6F_5/Cl	C_6F_5	Cl
Mes/BzO	1,3,5-$(CH_3)_3$-C_6H_2	$C_6H_5CO_2$
Mes/TsO	1,3,5-$(CH_3)_3$-C_6H_2	$C_6H_5SO_3$

Figure 1. Iodosylarene adducts and their abbreviations that are investigated in this study. Molecular structure of **Mes/Cl**, reproduced from the previous X-ray crystal structure.

(Cl in this case), which is bound to the I(III) atom upon the formation of the iodosylmesitylene adduct, emerges as an important structural factor, in addition to iodosylarene substituents. In the present paper, we prepared iodosylarene adducts with various arenes and anions on I(III) and investigated structure−reactivity relationships. The present study shows that iodosylarene adducts of manganese(IV) salen complexes are not just a precursor to active high-valent manganese−oxo species but are indeed an active oxygen-atom-transfer reagents, consistent with our previous communication.[15] Furthermore, the present study clarifies that the reactivity and selectivity of iodosylarene adducts are critically dependent on steric and electronic properties of the arenes and anions on I(III) of the coordinated iodosylarenes.

RESULTS AND DISCUSSION

Preparation and Characterization of Iodosylarene Adducts. Among iodosylarene adducts that are listed in Figure 1, the synthesis of **Ph/Cl** and **Mes/Cl** was already reported.[15] **$Et_3C_6H_2$/Cl** and **C_6F_5/Cl** was prepared exactly in the same manner. **Mes/BzO** and **Mes/TsO** were obtained from **Mes/Cl** by the reaction with 10 equiv of AgBzO and 2 equiv of AgTsO, respectively. Precipitation in CH_2Cl_2−pentane solution at −20 °C gave analytically pure iodosylarene adducts. Because of instability, **Mes/TsO** was utilized without purification, but ^{1}H NMR shows that the CH_2Cl_2 solution of **Mes/TsO** is sufficiently pure as compared with the other iodosylarene adducts (vide infra).

Figure 2 shows ^{1}H NMR and EPR (electron paramagnetic resonance) spectra of **$Et_3C_6H_2$/Cl**. Data of the other iodosylarene adducts are included in the Supporting Information (Figure S1 and S2). **$Et_3C_6H_2$/Cl** shows three ^{1}H

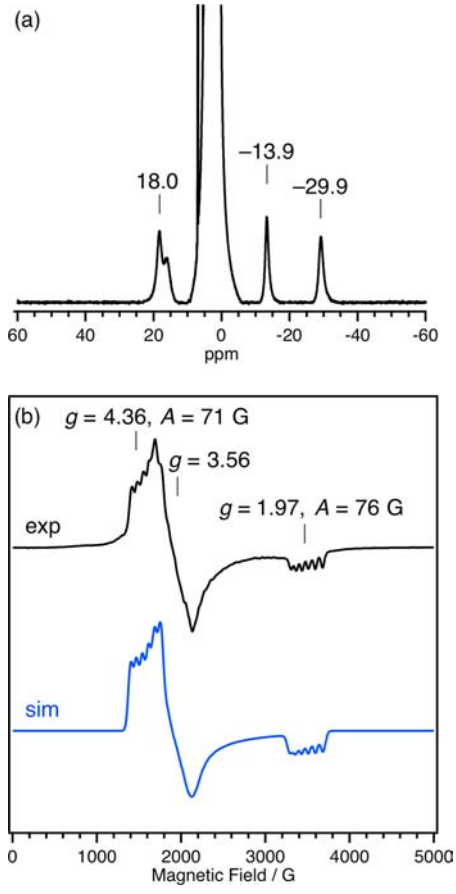

Figure 2. (a) ^{1}H NMR spectrum of **$Et_3C_6H_2$/Cl** (10 mM) in CD_2Cl_2 at 273 K. (b) EPR spectrum of **$Et_3C_6H_2$/Cl** (10 mM) in frozen CH_2Cl_2 at 4 K (black line). (conditions) Microwave frequency, 9.657 GHz; microwave power, 1.00 mW; modulation amplitude, 7 G; time constant, 163.84 ms; conversion time, 163.84 ms. The blue line is a simulation curve with *g* values and Mn hyperfine parameters as indicated.

dx.doi.org/10.1021/ic401270j | *Inorg. Chem.* 2013, 52, 9557−9566

NMR signals at 18.0, −13.9, and −30.3 ppm, which are almost the same as those for crystallographically characterized **Mes/Cl** (18.5, −13.6, and −29.7 ppm).[15] These ^{1}H NMR features are similar to those of the $Mn^{IV}(salen)(L)_2$ complexes (L = CF_3CH_2O, N_3, Cl), and the signals at 18.0 and −13.9 ppm were assigned as arising from the phenolate protons.[18] The other iodosylarene adducts also show three ^{1}H NMR signals at similar positions, and no other signal is observed at all, indicating all the iodosylarene adducts are prepared in pure form, irrespective of the difference of arenes and anions. **$Et_3C_6H_2$/Cl** and the other iodosylarene adducts show intense EPR signals that are characteristic for the $S = 3/2$ system, indicative of the manganese(IV) oxidation state. The signals at $g = 4.36$ and 1.97 show a six-line hyperfine splitting with $A = 71$ and 76 G, respectively, arising from the $I = 5/2$ ^{55}Mn nucleus.

As shown in Figure 3a, the absorption spectrum of **$Et_3C_6H_2$/Cl** is similar to that of crystallographically characterized **Mes/Cl**.[15] **$Et_3C_6H_2$/Cl** shows an intense CD (circular dichroism) signal in the region from 200 to 350 nm (Figure 3b). Similar absorption and CD features are observed for the other iodosylarene adducts (Figure S3 and S4, Supporting Information). As previously shown by X-ray diffraction and CD studies, the intense CD signal in this region is indicative of the formation of a stepped conformation,[18] which is also the case for **Mes/Cl** in Figure 1.[15] Thus, CD data indicate that the iodosylarene adducts prepared in this study also adopt a stepped conformation.

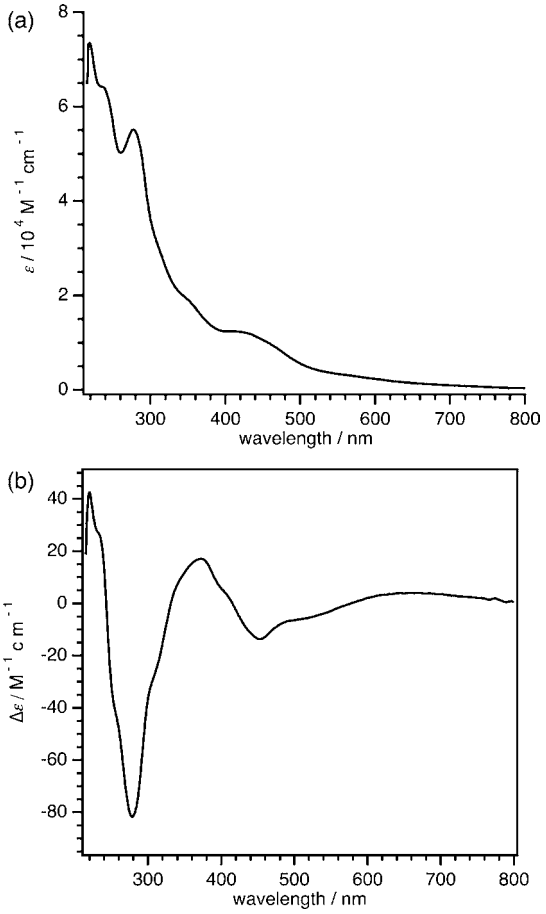

Figure 3. (a) Absorption and (b) CD spectra of **$Et_3C_6H_2$/Cl** (0.2 mM, 0.1 cm cell) in CH_2Cl_2 at room temperature.

ESI (electrospray ionization) mass spectra were measured to confirm the composition of the iodosylarene adducts. As shown in Figure 4b, the CH_2Cl_2 solution of **$Et_3C_6H_2$/Cl** shows a main signal at m/z 1242.42, which is assigned as arising from the $[\mathbf{Et_3C_6H_2/Cl} - Cl]^+$ ion. This assignment is supported by the comparison of experimental and calculated isotope distribution patterns of $[\mathbf{Et_3C_6H_2/Cl} - Cl]^+$ (Figure 4a). Furthermore, after vigorously stirring the CH_2Cl_2 solution of **$Et_3C_6H_2$/Cl** in the presence of $H_2{}^{18}O$ for 2 h, the ion signal at m/z 1242.42 is shifted by 4 Da to m/z 1246.05 (Figure 4c), indicating that this molecular ion contains two H_2O-exchangable oxygen atoms, consistent with the coordination of two iodosylarenes.[19] The compositions of the other iodosylarene adducts were also confirmed by ESI mass spectrometry (Figure S5 and S6, Supporting Information).

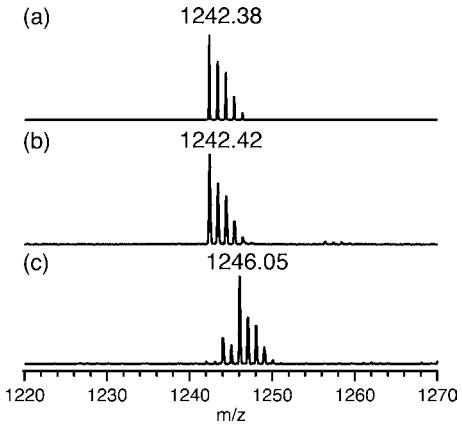

Figure 4. ESI mass spectra of **$Et_3C_6H_2$/Cl** in CH_2Cl_2 (b) before and (c) after exposure to $H_2{}^{18}O$. The cone voltage is 40 V. (a) Calculated isotope distribution pattern for $[\mathbf{Et_3C_6H_2/Cl} - Cl]^+$ ($C_{60}H_{86}ClI_2MnN_2O_4$). The spectra in the full range are shown in Figure S6 (Supporting Information).

Interestingly, the electrospray ionization gives ion signals that correspond to the formally manganese(VI) oxo species, in addition to the adduct ion, as shown in Figure 5 ("oxo-ion" and "adduct-ion" in Scheme 1). It was confirmed that the m/z values of these oxo-ions are shifted by 4.0 Da upon exposure to $H_2{}^{18}O$ (Figure S7, Supporting Information). But these oxo-ions are mostly attributed to an artifact that is only generated upon the electrospray ionization, because ^{1}H NMR, EPR, IR, and absorption studies do not show any detectable amount of the manganese(VI) oxo species. Relative intensities of oxo-ions compared with those of adduct-ions increase in the order **$Et_3C_6H_2$/Cl ~ Mes/Cl < Ph/Cl ≪ C_6F_5/Cl**. It is also shown that relative intensities of oxo-ions increase in the order **Mes/BzO < Mes/Cl ≪ Mes/TsO**. This order is roughly in parallel with an increasing order of the pK_a values (BzOH, 11; HCl, 2.0; TsOH, 0.9 in DMSO[20]). The difference of ESI mass spectra is seemingly correlated with the difference of I−OMn bond strength, as suggested from the IR study (vide infra).

Figure 6 shows IR spectra of **$Et_3C_6H_2$/Cl** and ^{18}O-labeled **$Et_3C_6H_2$/Cl**. The ^{18}O content of the ^{18}O-labeled sample was found to be about 80%, as estimated from ESI mass spectrometry (Figure 4). We observe quite broad $^{16}O/^{18}O$ isotope-sensitive bands that are only slightly separated. The same holds true for the other iodosylarene adducts (Figures S8−S12, Supporting Information). For this reason, the difference spectrum between ^{16}O- and ^{18}O-samples gave

dx.doi.org/10.1021/ic401270j | Inorg. Chem. 2013, 52, 9557−9566

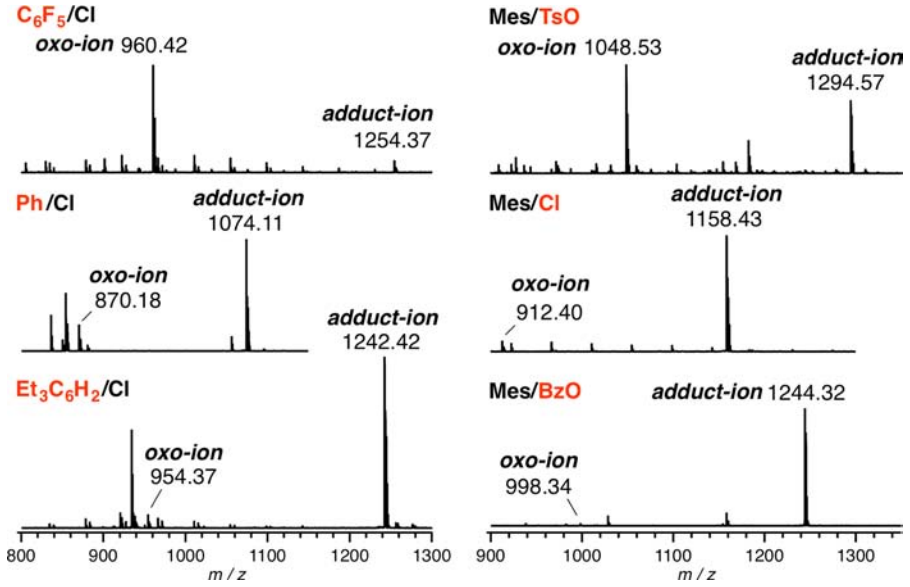

Figure 5. ESI mass spectra of the iodosylarene adducts under the same measurement conditions in CH_2Cl_2 at the cone voltage of 40 V. The ion signals denoted with "adduct-ion" and "oxo-ion" are shown in Scheme 1.

Scheme 1

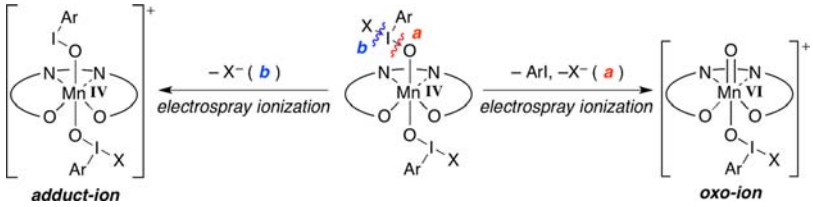

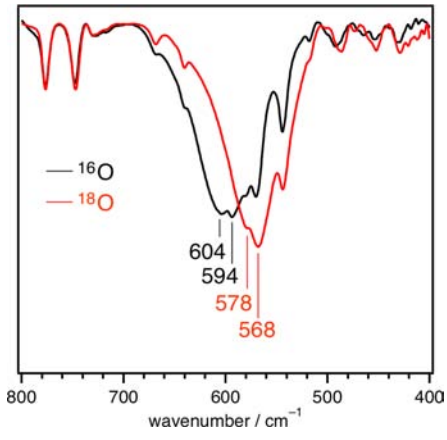

Figure 6. IR spectra (KBr pellet) of $Et_3C_6H_2$/**Cl** (black line) and ^{18}O-labeled $Et_3C_6H_2$/**Cl** (red line).

unclear results in determining the positions of the isotope-sensitive bands. We thus carefully pinpoint the $^{16}O/^{18}O$ isotope-sensitive bands from the original data, consulting density functional theory (DFT) calculations (vide infra). $Et_3C_6H_2$/**Cl** apparently shows two $^{16}O/^{18}O$ isotope-sensitive bands at 604 and 594 cm^{-1}, which are shifted to 578 and 568 cm^{-1} upon the ^{18}O labeling, respectively. The $^{16}O/^{18}O$ isotope-sensitive bands for the other iodosylarene adducts are summarized in Table 1. Table 1 lists the revised values for **Mes**/**Cl** and **Ph**/**Cl**, because these are previously determined from difference spectra between ^{16}O- and ^{18}O-samples.[15] In addition to $Et_3C_6H_2$/**Cl**, **Mes**/**TsO** also shows two $^{16}O/^{18}O$ isotope-sensitive bands, while the other iodosylarene adducts seemingly show a single isotope-sensitive band. Two $^{16}O/^{18}O$ isotope-sensitive bands in $Et_3C_6H_2$/**Cl** and **Mes**/**TsO** might arise from the difference of coordination environments of two iodosylarene moieties, or different IR vibrations indicated by DFT calculations (vide infra). In the case of C_6F_5/**Cl**, the ^{18}O-labeled sample could not be prepared because of decomposition upon exposure to $H_2{}^{18}O$, and then, the IR band at 625 cm^{-1} is tentatively assigned as the corresponding band (Figure S12, Supporting Information).

Table 1. $^{16}O/^{18}O$ Isotope-Sensitive IR Bands in Iodosylarene Adducts[a]

	^{16}O adduct (cm^{-1})	^{18}O adduct (cm^{-1})	$^{16}O - {}^{18}O$ (cm^{-1})
C_6F_5/Cl	625	*b*	*b*
Ph/Cl	590	568	−22
$Et_3C_6H_2$/Cl	604/594	578/568	−26/−26
Mes/TsO	639/634	612/608	−27/−26
Mes/Cl	607	577	−30
Mes/BzO	609	586	−23

[a]The IR spectrum of $Et_3C_6H_2$/**Cl** is shown in Figure 6. The IR spectra of the other iodosylarene adducts are shown in Figures S8−S12 (Supporting Information). [b]^{18}O-labeled C_6F_5/**Cl** could not be prepared because of decomposition upon exposure to $H_2{}^{18}O$ in CH_2Cl_2.

In order to assign $^{16}O/^{18}O$ isotope-sensitive IR bands, we conducted DFT calculations for **Mes**/**Cl** and C_6F_5/**Cl**, in which the X-ray structure of **Mes**/**Cl** was modified to construct symmetric structures suitable for calculations. Table 2 lists

dx.doi.org/10.1021/ic401270j | Inorg. Chem. 2013, 52, 9557−9566

Table 2. DFT-Calculated $^{16}O/^{18}O$ Isotope-Sensitive IR Bands for Mes/Cl and C_6F_5/Cl[a]

	calcd IR shift (intensity)/cm^{-1}			
	Mes/Cl		C_6F_5/Cl	
^{16}O	688 (1320)	695 (830)	682 (1010)	716 (870)
^{18}O	646 (100)	663 (1780)	664 (1560)	715 (100)
isotope shift (corrected[b])/cm^{-1}	−42 (−37)	−32 (−28)	−18 (−16)	−1 (−0.9)

[a]The vibration mode is shown in Figure S13 (Supporting Information). [b]For the purpose of comparison with the experimental isotope shifts, the calculated isotope shifts were corrected by adjusting the calculated IR shifts to the experimental value (**Mes/Cl**, 607 cm^{-1}; **C_6F_5/Cl**, 625 cm^{-1}) with appropriate scaling factors.

calculated $^{16}O/^{18}O$ isotope-sensitive IR bands. The calculations indicate that these isotope-sensitive IR bands originate from the O−Mn−O antisymmetric stretching (Figure S13, Supporting Information), in contrast to the erroneous assignment as the triatomic Mn−O−I stretching in our previous communication.[15] Both **Mes/Cl** and **C_6F_5/Cl** show two O−Mn−O antisymmetric stretching bands, because of mixing with the angle bending motion of the O−I−Ar moiety. The averaged shift position of **C_6F_5/Cl** (699 cm^{-1}) is more shifted to higher frequency than the averaged shift position of **Mes/Cl** (692 cm^{-1}), consistent with the experimental observation in Table 1. For the purpose of comparison with the experimental isotope shifts, the calculated isotope shifts were corrected by adjusting the calculated IR shifts to the experimental value (**Mes/Cl**, 607 cm^{-1}; **C_6F_5/Cl**, 625 cm^{-1}) with appropriate scaling factors. The obtained value of −33 cm^{-1} as an averaged value for **Mes/Cl** is consistent with the assignment of the experimental isotope shift in Table 1. The experiments show that this O−Mn−O antisymmetric stretching bands of **Mes/TsO** and **C_6F_5/Cl** appear at higher frequency, indicative of a stronger M−O bond.

According to the spectroscopic data described in this section, all the iodosylarene adducts are successfully prepared in a pure form. High-valent manganese−oxo species are not detected in any significant amount. The iodosylarene adducts have a manganese(IV) center in common, as indicated by EPR spectroscopy. ESI mass spectrometry shows that the present iodosylarene adducts carry two iodosylarene molecules as external axial ligands. ESI mass spectra also show that the Cl anion in **Mes/Cl** is replaced by the BzO or TsO anion in **Mes/BzO** and **Mes/TsO**, respectively. In the X-ray crystal structure of **Mes/Cl**, the Cl anions are bonded to I(III) of the coordinated iodosylmesitylene.[15] But it is not clear from the present solution studies whether the anions including Cl, BzO, and TsO are bonded to I(III) also in solution. CD spectroscopy suggests that all the iodosylarene adducts most probably adopt a stepped conformation, as is observed for **Mes/Cl** shown in Figure 1.

Stoichiometric Sulfoxidation and Epoxidation by Iodosylarene Adducts of a Manganese(IV) Salen Complex. The reactivity of the present iodosylarene adducts for thioanisole was investigated. Figure 7a shows absorption spectral changes of **$Et_3C_6H_2$/Cl** recorded after the addition of thioanisole at 293 K. The absorption at 690 nm increases during the first 200 min and then decreases thereafter (Figure 7b). This 690 nm-absorption is assigned as arising from the $Mn^{IV}(salen)(Cl)_2$ complex.[18b] Scheme 2 shows the most probable reaction pathway. But the actual kinetic traces in Figure 7b show additional complications, especially the inflections of the data that are commonly observed for the reactions of **C_6F_5/Cl**, **Ph/Cl**, **Mes/Cl**, and **$Et_3C_6H_2$/Cl** with thioanisole. These anomalies could not be explained by the model in Scheme 2. The bis-adduct transfers one of two active

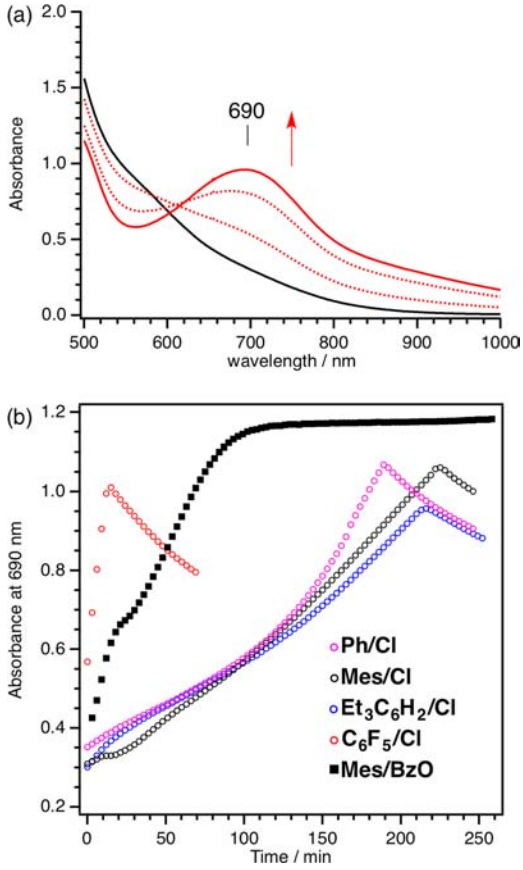

Figure 7. (a) Absorption spectral changes of **$Et_3C_6H_2$/Cl** (0.3 mM, 0.1 cm cell) in the course of the reaction with thioanisole (156 mM) at 293 K in CH_2Cl_2. The absorption at 690 nm comes from $Mn^{IV}(salen)(Cl)_2$ (Scheme 2). (b) Kinetic traces at 690 nm for **Ph/Cl** (purple circle), **Mes/Cl** (black circle), **$Et_3C_6H_2$/Cl** (blue circle), and **C_6F_5/Cl** (red circle). Kinetic traces shown by black squares are absorption changes at 655 nm for **Mes/BzO**. Absorption spectral changes in the reaction of **Mes/BzO** with thioanisole are shown in Figure S14 (Supporting Information).

oxygen atoms to thioanisole to afford the monoadduct, which then transfers the second oxygen atom, generating $Mn^{IV}(salen)(Cl)_2$. This two-step process corresponds to the increase of the 690-nm absorption over 200 min. The absorption spectral changes from **$Et_3C_6H_2$/Cl** to $Mn^{IV}(salen)(Cl)_2$ do not show isosbestic points, and there is no sign of buildup of the monoadduct. This suggests that the bis-adduct and the monoadduct have similar reactivity. The subsequent decrease of the 690-nm absorption is ascribed to the decomposition of $Mn^{IV}(salen)(Cl)_2$ to $Mn^{III}(salen)(Cl)$ in the presence of an excess of thioanisole. Consistently, the rate for the decrease of the 690-nm absorption is almost the same

dx.doi.org/10.1021/ic401270j | Inorg. Chem. 2013, 52, 9557−9566

Scheme 2

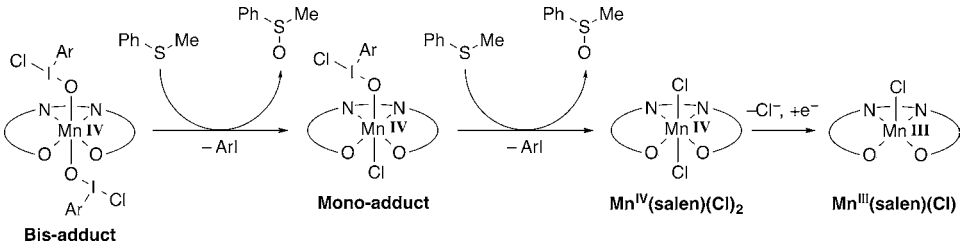

Table 3. Stoichiometric Oxidation of Thioanisole and Styrenes by Iodosylarene Adducts[a]

substrate		thioanisole	styrene	*cis*-β-methyl styrene		*trans*-β-methyl styrene
product		methyl phenyl sulfoxide	styrene oxide	*cis*-β-methyl styrene oxide	*trans*-β-methyl styrene oxide	*trans*-β-methyl styrene oxide
ee % (yield %)	C_6F_5/Cl	0 (90)	64 ± 2 (22)	48 ± 1 (38)	21 ± 5 (6)[b]	54 ± 2 (88)
	Ph/Cl	6 ± 1 (38)	21 ± 5 (26)	44 ± 1 (10)	27 ± 1 (12)[c]	22 ± 3 (23)
	$Et_3C_6H_2$/Cl	0 (71)	31 ± 1 (36)	63 ± 1 (10)	22 ± 1 (10)[c]	31 ± 1 (56)
	Mes/TsO	4 ± 1 (63)	33 ± 1 (14)	48 ± 1 (34)	14 ± 3 (4)[c]	30 ± 1 (48)
	Mes/Cl	3 ± 1 (49)	52 ± 1 (20)	63 ± 1 (25)	27 ± 4 (8)[c]	41 ± 1 (47)
	Mes/BzO	35 ± 1 (61)	20 ± 1 (89)	48 ± 1 (19)	32 ± 1 (41)[c]	22 ± 1 (61)
config		*S*	*R*	1*R*,2*S*	1*R*,2*R*;[b] 1*S*,2*S*[c]	1*R*,2*R*

[a]The enantiomeric excesses and the yields are the averaged values from three independent experiments. Yields are based on the manganese-bound iodosylarene. [b](1*R*,2*R*)-*trans*-β-Methylstyrene oxide is obtained as a product. [c](1*S*,2*S*)-*trans*-β-Methylstyrene oxide is obtained as a product.

for **Ph/Cl**, **Mes/Cl**, **$Et_3C_6H_2$/Cl**, and **C_6F_5/Cl**, all of which are expected to generate $Mn^{IV}(salen)(Cl)_2$ after the oxygen-atom transfer reactions.

In order to evaluate the effect of the iodosylarene substituent, absorption spectral changes for the same reactions were measured for **Ph/Cl**, **Mes/Cl**, **$Et_3C_6H_2$/Cl**, and **C_6F_5/Cl** (Figure 7b). It is clearly shown that **C_6F_5/Cl** reacts with thioanisole much faster than **Ph/Cl**, **Mes/Cl**, and **$Et_3C_6H_2$/Cl**, indicating that the pentafluorophenyl group significantly accelerates the reaction. We also measured absorption spectral changes for the reaction with thioanisole by **Mes/BzO** and **Mes/TsO**, to investigate the effect of anions on I(III). The reaction of **Mes/BzO** with thioanisole gave a species with an absorption at 655 nm, which is assigned as arising from the $Mn^{IV}(salen)(BzO)_2$ complex (Figure S14, Supporting Information). The $Mn^{IV}(salen)(BzO)_2$ complex is apparently stable under the conditions, and the decay to the $Mn^{III}(salen)(BzO)$ complex is not observed, as seen from the absorption changes at 655 nm in Figure 7b. In contrast, the reaction of **Mes/TsO** with thioanisole very quickly affords the $Mn^{III}(salen)(TsO)$ complex without the formation of $Mn^{IV}(salen)(TsO)_2$ (Figure S15, Supporting Information). This is probably because the reaction of **Mes/TsO** with thioanisole might similarly give the $Mn^{IV}(salen)(TsO)_2$ complex, which decomposes more rapidly than the rate of formation. The kinetic traces qualitatively show that the reactivity of the iodosylarene adducts is accelerated in the order Cl < BzO < TsO. Quite interestingly, this order of reactivity is in parallel with the O–Mn–O antisymmetric stretching IR band (607, 609, and 639/634 cm^{-1} for **Mes/Cl**, **Mes/BzO**, and **Mes/TsO** as shown in Table 1). It is also shown that the O–Mn–O antisymmetric stretching band of reactive **C_6F_5/Cl** appears at 625 cm^{-1}, which is shifted to a higher frequency as compared with less reactive iodosylarene adducts such as **Ph/Cl** (590 cm^{-1}), **$Et_3C_6H_2$/Cl** (604/594 cm^{-1}), and **Mes/Cl** (607 cm^{-1}). This indicates that the high reactivity of **Mes/TsO** and **C_6F_5/Cl** is correlated with the Mn–O bond strength. The strong Mn–O bonds for **Mes/TsO** and **C_6F_5/Cl** suggest weak I–OMn bonds and strong electrophilicity of the I–O moiety, which are probably direct factors for their high reactivity.

The stoichiometric reactions of the iodosylarene adducts with 2.2 equiv of thioanisole afford methyl phenyl sulfoxide as a major product. As a control reaction, we carried out the reaction of iodosobenzene with thioanisole, which do not afford methyl phenyl sulfoxide at all. As shown in Table 3, only **Mes/BzO** bearing a BzO anion shows moderate enantioselectivity (35% ee), although the other iodosylarene adducts show negligibly small enantioselectivities (0–6% ee). Notably, the enantioselectivity of **Mes/TsO** is only 4% ee, indicating that the strong binding property of the BzO anion contributes to the selectivity.

We also attempted to investigate the reactivity of the iodosylarene adducts for styrenes and conducted single-turnover reactions of iodosylarene adducts with styrenes. But in the presence of styrenes, the decomposition of the $Mn^{IV}(salen)(X)_2$ products is much faster, which precludes us from precisely estimating the rate of reactions with styrenes.

The stoichiometric reactions of the iodosylarene adducts with styrenes afford styrene oxides. Benzaldehyde is also detected with ^1H NMR as a byproduct, but the yield of benzaldehyde is negligibly small. The control reaction of iodosobenzene with *cis*-β-methylstyrene did not afford epoxidation products at all. Table 3 summarizes the ee and the yield of the styrene oxide products. In the case of olefin epoxidation, all the iodosylarene adducts show moderate enantioselectivities, indicating that the olefin epoxidation is mechanistically different from sulfoxidation. Figure 8 illustrates the cis/trans ratios of the β-methylstyrene oxides in the stoichiometric epoxidation of *cis*-β-methylstyrene. The cis-to-trans isomerization is significantly suppressed in the epoxidation by **C_6F_5/Cl** and **Mes/TsO**, while the epoxidation by **Mes/BzO** enhances the cis-to-trans isomerization to afford *trans*-β-methylstyrene oxide as a major product.

dx.doi.org/10.1021/ic401270j | *Inorg. Chem.* 2013, 52, 9557–9566

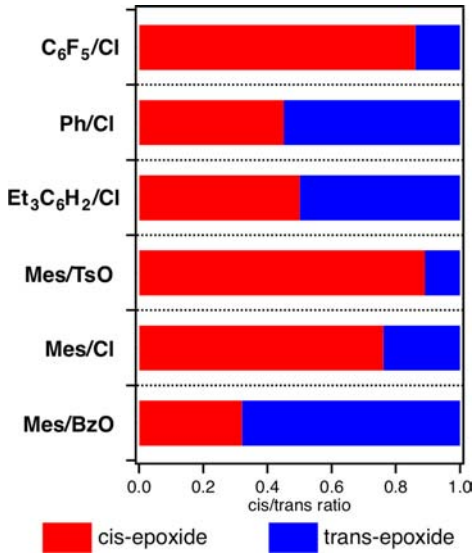

Figure 8. Cis/trans ratios of the *β*-methylstyrene oxides in the stoichiometric epoxidation of *cis-β*-methylstyrene.

We then investigated the effect of the arene moiety of the coordinated iodosylarene on enantioselectivity. **C_6F_5/Cl** is especially effective for the epoxidation of styrene (64% ee) among other substrates, as compared with **Ph/Cl**, **$Et_3C_6H_2$/Cl**, and **Mes/Cl** (21, 31, and 52% ee, respectively). We found a good correlation between the ee of styrene oxide and the ratio of *cis-β*-methylstyrene oxide in the epoxidation of *cis-β*-methylstyrene (Figure S16, Supporting Information). This is because the suppressed cis-to-trans isomerization, arising from the electron-withdrawing pentafluorophenyl group in the present case, directly contributes to the high enantioselectivity in the epoxidation of styrene.[21] **Mes/Cl** bearing a sterically hindered mesityl group shows higher enantioselectivity for every olefin than **Ph/Cl**, but more sterically demanding **$Et_3C_6H_2$/Cl** is less effective than **Mes/Cl**. This result suggests that the steric bulk in the iodosylarene moiety is not a sole factor to determine the enantioselectivity. Among three anions, the Cl anion affords the best enantioselectivities for all styrenes. The TsO and BzO anions, which bear quite different electronic properties, show a similar trend in enantioselective epoxidations. These results indicate that the effect of the anions on the enantioselectivity comes from steric factors, rather than electronic factors.

The present experiments show that the enantio- and diastereoselectivity are critically dependent on the arenes and anions on I(III) of the coordinated iodosylarenes. This result is a clear indication that the iodosylarene adducts of manganese(IV) salen complexes are not just precursors to another active oxidant such as high-valent manganese−oxo species but indeed function by themselves as an active oxidant. We found that the electron-withdrawing pentafluorophenyl group and the *p*-toluenesulfonate anion increase the diastereoselectivity in the epoxidation of *cis-β*-methylstyrene. But it is much more difficult to interpret the enantioselectivities, which are probably affected by both electronic and steric properties of iodosylarene adducts.

Previously, in catalytic oxygenations by manganese(III) salen and porphyrin complexes, several groups proposed iodosylarene adducts of manganese(III) complexes as a key intermediate.[5,11−13] Because the conversion from manganese(III) complexes to manganese(V)−oxo species is expected to be very facile, the role of iodosylarene adducts of manganese(III) complexes as active species is limited for the reaction with very reactive substrates, where the formation of manganese(V)−oxo species is the rate-determining step. In contrast, in the present iodosylarene adducts, the oxidation state of manganese is manganese(IV), not manganese(III). The formation of manganese(VI)−oxo species from the iodosylarene adducts of manganese(IV) complexes should be less efficient. Indeed, we successfully obtained iodosylarene adducts of manganese(IV) salen complexes in every case without any sign of the formation of manganese(VI)−oxo species. Thus, we expect that the iodosylarene adducts of manganese(IV) complexes play a more significant role in the present oxygenation reactions, although the contribution of high-valent manganese−oxo species could not be excluded. In the case of iodosylarene adducts of manganese(V)−oxo complexes,[9,10a] iodosylarene adducts would play an exclusive role, because the further oxidation of manganese(V)−oxo is unlikely.

We then compare the present stoichiometric reactions by isolated iodosylarene adducts with the catalytic reactions previously reported.[11,12c,22] In the stoichiometric epoxidation

Scheme 3

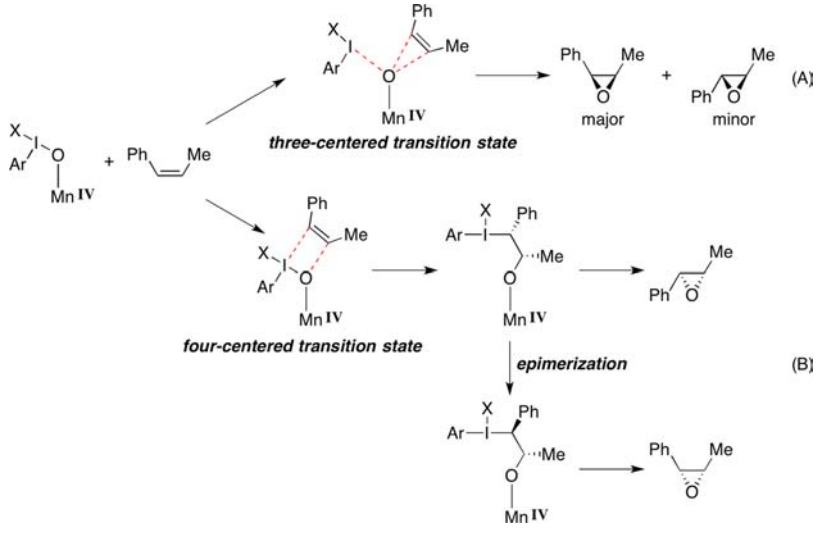

dx.doi.org/10.1021/ic401270j | Inorg. Chem. 2013, 52, 9557−9566

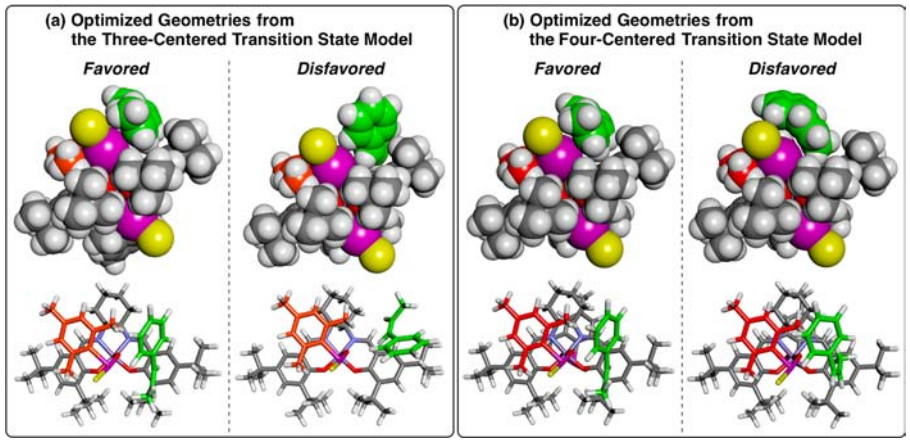

Figure 9. Optimized geometries of the **Mes/Cl**–*cis*-β-methylstyrene complex. (top) Space-filling representations from a side view. (bottom) Stick representations from a top view. DFT calculations were utilized to create these models. The favored structures are more stable than the disfavored structures by 2.1 and 1.4 kcal/mol in a and b, respectively. The energy of the favored structures in a and b is lower than the total energy of separated **Mes/Cl** and *cis*-β-methylstyrene by 10.2 and 10.8 kcal/mol, respectively.

of *cis*-β-methylstyrene by the present iodosylarene adducts of a manganese(IV) salen complex, the weakly binding TsO anion suppresses the cis-to-trans isomerization, while the strongly binding BzO anion enhances the cis-to-trans isomerization (Figure 8). The electron-withdrawing property and the steric hindrance of the iodosylarene moiety also alter the cis/trans ratio of the epoxide product. Interestingly, a similar trend is observed for catalytic epoxidations of stilbene by manganese(III) complexes with the same salen ligand[11,12c,22] and tetraphenylporphyrin.[22] The cis/trans ratio is significantly high for weakly binding anions such as BF_4^-, PF_6^-, and $CF_3SO_3^-$ as compared with the Cl anion. The use of C_6F_5IO and MesIO oxidants give a higher cis/trans ratio than the use of PhIO, which is also observed in the present stoichiometric epoxidation (Figure 8). In spite of the similarity in the cis-to-trans isomerization, the enantioselectivity trend in the epoxidation of styrene is apparently different. In the case of the present stoichiometric epoxidation, the enantioselectivity is increased in the order **Ph/Cl** < **Mes/Cl** < **C_6F_5/Cl** (Table 3). But in the catalytic epoxidation by Mn^{III}(salen)(Cl) using PhIO, MesIO, and C_6F_5IO as the oxidant, the difference of enantioselectivity is quite small.[12c] Therefore, the active species in catalytic epoxidation and the present iodosylarene adducts might be similar in the electronic properties that causes the cis-to-trans isomerization, but differ in the stereochemical property for enantioselective oxygen-atom transfer.

Proposed Mechanism for the Oxygen-Atom Transfer from the Iodosylarene Adducts. In the present study, we investigate stoichiometric reactions of purified iodosylarene adducts, to establish structure–selectivity relationships. Even under such simple conditions, the interpretation of enantioselectivity is not straightforward. We herein examine two possible pathways shown in Scheme 3. One of the pathways is the oxygen-atom transfer to olefins via the three-centered transition state, in which the ArIX moiety is leaving as the olefin approaches to the oxygen atom on manganese (path A). The path A is expected to give *cis*-β-methylstyrene oxide as a major product upon the epoxidation of *cis*-β-methylstyrene. Another pathway is the addition–elimination mechanism via the four-centered transition state (path B). Valentine et al. also proposed a similar mechanism for the metal-catalyzed oxygenation using iodosylarenes as a terminal oxidant.[6] In this mechanism, the elimination of ArIX and a manganese salen complex without epimerization releases *trans*-β-methylstyrene oxide. The *cis*-β-methylstyrene oxide could be obtained after the epimerization at the carbon center adjacent to ArIX.

We then created optimized geometries for the complexes between **Mes/Cl** and *cis*-β-methylstyrene, using the crystal structure of **Mes/Cl**[15] and DFT calculations. Figure 9a shows optimized **Mes/Cl**–*cis*-β-methylstyrene structures, which are obtained from the starting geometries where the C–C double bond of *cis*-β-methylstyrene is positioned in a perpendicular orientation to the I–O bond of the iodosylarene adduct. We also employ other starting geometries where the C–C double bond of *cis*-β-methylstyrene is positioned in a parallel orientation to the I–O bond of the iodosylarene adduct, which are intended to model the four-centered transition state. But the geometry optimization affords a pair of optimized structures in Figure 9b, which are essentially the same as those obtained in Figure 9a. The distance between **Mes/Cl** and *cis*-β-methylstyrene, which is 3.6–4.4 Å in these optimized structures, is shortened leading to the three-centered transition state (path A in Scheme 3). We assume that the order of energy between favored and disfavored structures would be maintained in the transition-state structures, because steric interactions between **Mes/Cl** and *cis*-β-methylstyrene are not altered significantly when *cis*-β-methylstyrene comes closer to the iodosylarene adduct. As illustrated in Figure 10, the **Mes/Cl**–

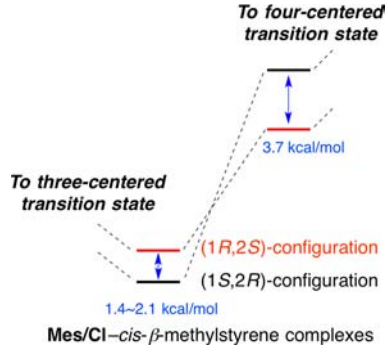

Figure 10. Energy diagram for the reaction of **Mes/Cl** with *cis*-β-methylstyrene to generate *cis*-β-methylstyrene with (1*R*,2*S*)-configuration as a major enantiomer.

dx.doi.org/10.1021/ic401270j | *Inorg. Chem.* 2013, 52, 9557–9566

cis-β-methylstyrene complex that affords *cis*-β-methylstyrene oxide with (1*S*,2*R*)-configuration is more stable by 2.1 and 1.4 kcal/mol in optimized structures in Figure 9a and b, respectively. But the (1*S*,2*R*)-configuration of *cis*-β-methylstyrene oxide is opposite to the experimental observation in Table 3. We then created models for the four-centered transition state (path B in Scheme 3) by introducing constraints between *cis*-β-methylstyrene and **Mes/Cl**, so as to position the C−C double bond of *cis*-β-methylstyrene in a parallel orientation to the I−O bond of the iodosylarene adduct. In this case, the adduct−substrate complex leading to *cis*-β-methylstyrene oxide with (1*R*,2*S*)-configuration is favored by 3.7 kcal/mol (Figure S17, Supporting Information). The (1*R*,2*S*)-configuration of *cis*-β-methylstyrene is the same as the experimental observation in Table 3, as illustrated in Figure 10.

■ CONCLUSION

We herein describe the effect of the arenes and anions on I(III) in iodosylarene adducts of a manganese(IV) salen complex on their reactivity and selectivity. It is shown that the electron-withdrawing pentafluorophenyl group and the *p*-toluenesulfonate anion on I(III) significantly accelerates the oxygen-atom transfer. Stoichiometric reactions with styrenes show that both enantioselectivity and diastereoselectivity are dependent on the arenes and anions on I(III) of the coordinated iodosylarenes. This observation is a clear indication that iodosylarene adducts of manganese(IV) salen complexes are not just precursors to active high-valent manganese−oxo species, but are indeed active oxygen-atom-transfer reagents. The present study clarifies that the reactivity and selectivity of iodosylarene adducts are regulated by both steric and electronic properties.

■ EXPERIMENTAL SECTION

Instrumentation. UV−vis spectra were recorded in CH_2Cl_2 in a quartz cell (l = 0.1 cm) on an Agilent 8453 spectrometer (Agilent Technologies). CD spectra were recorded in CH_2Cl_2 in a quartz cell (l = 0.1 cm) on a J-720W spectropolarimeter (JASCO). Measurements were done under the following conditions: scan rate, 100 nm min^{-1}; bandwidth, 5.0 nm; response, 4 s; resolution, 1 nm. EPR spectra were recorded for 50 μL of the frozen CH_2Cl_2 solution in a quartz cell (d = 5 mm) on an E500 continuous wave X-band spectrometer (Bruker) with an ESR 910 helium-flow cryostat (Oxford Instruments). Measurements were made under the following conditions: microwave frequency, 9.657 GHz; microwave power, 1.006 mW; modulation amplitude, 7 G; time constant, 163.84 ms; conversion time, 163.84 ms. Simulations of EPR spectra were done by using the EasySpin program.[23] 500 MHz ^{1}H NMR spectra were measured on an LA-500 spectrometer (JEOL). ^{1}H NMR chemical shifts in CD_2Cl_2 and $CDCl_3$ were referenced to $CHDCl_2$ (5.32 ppm) and $CHCl_3$ (7.24 ppm), respectively. ^{1}H NMR spectroscopy was utilized for the product analysis in the reactions of the iodosylarene adducts with thioanisole and styrenes. The ^{1}H NMR spectra of sulfoxide, sulfone, and epoxide products were reported, previously. Elemental analyses were conducted on a CHN corder MT-6 (Yanaco). ESI mass spectra were obtained with a LCT time-of-flight mass spectrometer equipped with an electrospray ionization interface (Micromass). GC-MS analysis was run on a QP-5000 GC-MS system (Shimadzu) equipped with a capillary gas chromatography (GC-17A, CBP5-M25-025 capillary column). Enantiomeric excesses were determined by GC (GC-2014, Shimadzu) using Astec CHIRALDEX G-TA fused silica capillary column (30 m × 0.25 mm × 0.12 μm film thickness). GC chromatograms of epoxides were reported previously.[15] IR spectra were recorded for the KBr pellet on a FT-IR-6100 (JASCO) spectrophotometer. IR spectra were measured for the KBr pellet on an FT/IR-6100 (JASCO).

Materials. Anhydrous solvents were purchased from Kanto or Wako and were utilized as received. CD_2Cl_2 and $CDCl_3$ were purchased from ACROS and were passed through aluminum oxide just before use. (*R*,*R*)-*N*,*N*-bis(3,5-di-*tert*-butylsalicylidene)-1,2-cyclohexanediamino manganese(III) chloride, *trans*-β-methylstyrene, and (1*S*,2*S*)-*trans*-β-methylstyrene oxide were purchased from Aldrich and were used as received. *m*-CPBA (*m*-choloroperoxybenzoic acid) was purchased from Nacalai. *Cis*-β-methylstyrene, (*R*)-styrene oxide, methyl phenyl sulfide, methyl phenyl sulfoxide, methyl phenyl sulfone, sodium perborated tetrahydrate and ceric ammonium nitrate were purchased from Wako. $CHCl_2CHCl_2$, PhIO and [bis-(trifluoroacetoxy)iodo]pentafluorobenzene, 1,3,5-triethylbenzene, and tetrabutylammonium iodide were purchased from TCI. Sodium sulfite was purchased from Kanto. Silver benzoate and silver tosylate were purchased from Aldrich. Pentafluoroiodosylbenzene[24] and triethyliodosylbenzene[8b] were prepared according to the literature procedures. The $Mn^{IV}(salen)(Cl)_2$ complex from Jacobsen's manganese salen complex was prepared according to our previously reported method.[25] Synthesis of **Mes/Cl** and **Ph/Cl** were reported in our previous paper.[15]

Synthesis of $Et_3C_6H_2$/Cl. To a solution of $Mn^{IV}(salen)(Cl)_2$ (15 mg, 0.0225 mmol) in anhydrous CH_2Cl_2 (1 mL) was added 10 equiv of triethyliodosylbenzene (68 mg, 0.225 mmol) at room temperature. The mixture was stirred for about 10 min, and the resulting solution was passed through a membrane filter (Millex-FG, poresize 0.20 μm, diameter 25 mm, Millipore). The addition of hexane and standing the biphasic solution at −20 °C overnight gave the analytically pure Et_3PhIO adduct. Anal. calcd for $C_{60}H_{86}Cl_2I_2MnN_2O_4\cdot(H_2O)_{1.8}$: C, 54.95; H, 6.89; N, 2.14. Found: C, 54.78; H, 6.60; N, 2.02.

Synthesis of C_6F_5/Cl. To a solution of $Mn^{IV}(salen)(Cl)_2$ (90 mg, 0.135 mmol) in anhydrous CH_2Cl_2 (3 mL) was added 5 equiv of pentafluoroiodosylbenzene (210 mg, 0.675 mmol) at room temperature. After the mixture was stirred for 20 min, the green-brown solution was filtered through a membrane filter (Millex-FG, pore size 0.20 μm, diameter 25 mm, Millipore) to remove excess pentafluoroiodosylbenzene. The addition of excess anhydrous pentane (50 mL) at room temperature and standing the biphasic solution overnight at −20 °C gave a green-brown precipitate as analytically pure sample (151 mg, 0.117 mmol) in 87% yield. Anal. Calcd for $C_{48}H_{52}Cl_2F_{10}I_2MnN_2O_4\cdot(H_2O)\cdot(C_6H_5I)_{0.4}$: C, 42.44; H, 3.82; N, 1.96. Found: C, 42.16; H, 3.90; N, 1.89.

Synthesis of Mes/BzO. To the solution of **Mes/Cl** (82.5 mg, 0.069 mmol) in anhydrous CH_2Cl_2 (4 mL) was added 10 equiv of AgOBz (156 mg, 0.669 mmol) at 233 K. The resulting solution was stirred for 3 h at 233 K. Then, the cold solution was filtered to remove silver salts and was subsequently passed through a membrane filter (Millex-FG, poresize 0.20 μm, diameter 25 mm, Millipore). The resulting solution was evaporated in vacuo at 233 K. Recrystallization from toluene and hexane at 243 K gave a red brown precipitate as an analytically pure sample (92.1 mg, 0.067 mmol) in 97% yield. Anal. calcd for $C_{68}H_{84}I_2MnN_2O_8\cdot(H_2O)$: C, 59.01; H, 6.26; N, 2.02. Found: C, 59.09; H, 6.24; N, 2.00.

Synthesis of Mes/TsO. To the solution of **Mes/Cl** (26.8 mg, 0.0225 mmol) in anhydrous CH_2Cl_2 (0.5 mL) was added 2 equiv of AgOTs (12.7 mg, 0.045 mmol) at 233 K. The resulting solution was stirred for 3 h at 233 K. Then, the cold solution kept at 233 K was passed through a membrane filter (Millex-FG poresize 0.20 μm, diameter 25 mm, Millipore). **Mes/TsO** is found to be unstable under ambient conditions and is thus utilized for the reactivity study without purification.

Typical Procedure for Stoichiometric Epoxidations of Styrenes by Isolated Iodosylarene Adducts. To a solution of **$Et_3C_6H_2$/Cl** (28.7 mg, 0.0225 mmol) in anhydrous CH_2Cl_2 (0.5 mL) was added 2.2 equiv of styrene (5.6 μL, 0.0495 mmol). The mixture was stirred for 5 h at room temperature, and then, the solvent was removed by rotary evaporation. The residue was dissolved in the solvent mixture (hexane/diethyl ether = 20:1, 20 mL) and was passed through a pad of silica gel. The enantiomeric excesses are determined by GC analysis. The yield was determined by ^{1}H NMR spectroscopy using $CHCl_2CHCl_2$ as the internal standard.

dx.doi.org/10.1021/ic401270j | Inorg. Chem. 2013, 52, 9557−9566

Typical Procedure for Stoichiometric Epoxidations of Styrenes by in Situ Generate Mes/TsO. To the solution of **Mes/Cl** (26.8 mg, 0.0225 mmol) in anhydrous CH_2Cl_2 (0.5 mL) were added 2 equiv of AgOTs (12.7 mg, 0.045 mmol) at 233 K. The resulting solution was stirred for 3 h at 233 K. Then the cold solution kept at 233 K was passed through a membrane filter (Millex-FG, poresize 0.20 μm, diameter 25 mm, Millipore). To this freshly prepared solution of **Mes/TsO** was added 2.2 equiv of styrene (5.6 μL, 0.0495 mmol). The mixture was stirred for 5 h at room temperature, and then, the solvent was removed by rotary evaporation. The residue was dissolved in the solvent mixture (hexane/diethyl ether = 20:1, 20 mL) and was passed through a pad of silica gel. The enantiomeric excesses were determined by GC analysis. The yield was determined by ^{1}H NMR spectroscopy using $CHCl_2CHCl_2$ as the internal standard.

Typical Procedure for Stoichiometric Sulfoxidations of Thioanisole by Isolated Iodosylarene Adducts. To a solution of **$Et_3C_6H_2$/Cl** (28.7 mg, 0.0225 mmol) in anhydrous CH_2Cl_2 (0.5 mL) was added 2.2 equiv of thioanisole (6.0 μL, 0.0495 mmol). The mixture was stirred for 5 h, and the solvent was removed by rotary evaporation. The residue dissolved in CH_3CN was passed through a pad of wakogel50C18 (38−63 μm) to give methyl phenyl sulfoxide as a major product. The enantiomeric excess was determined by GC analysis. The yield was determined by ^{1}H NMR spectroscopy using $CHCl_2CHCl_2$ as the internal standard.

Typical Procedure for Stoichiometric Sulfoxidations of Thioanisole by in Situ Generate Mes/TsO. To the solution of **Mes/Cl** (26.8 mg, 0.0225 mmol) in anhydrous CH_2Cl_2 (0.5 mL) were added 2 equiv of AgOTs (12.7 mg, 0.045 mmol) at 233 K. The resulting solution was stirred for 3 h at 233 K. Then, the cold solution kept at 233 K was passed through a membrane filter (Millex-FG, poresize 0.20 μm, diameter 25 mm, Millipore). To this freshly prepared solution of **Mes/TsO** was added 2.2 equiv of thioanisole (6.0 μL, 0.0495 mmol). The mixture was stirred for 5 h at room temperature, and then, the solvent was removed by rotary evaporation. The residue dissolved in CH_3CN was passed through a pad of wakogel50C18 (38−63 μm) to give methyl phenyl sulfoxide as a major product. The enantiomeric excesses are determined by GC analysis. The yield was determined by ^{1}H NMR spectroscopy using $CHCl_2CHCl_2$ as the internal standard.

DFT Calculations. DFT calculation was performed using the Gaussian 09 program package. The optimized structures and the vibrational frequencies were calculated using LC-BLYP density functional methods. The basis sets used were 6-311G(d) augmented by diffuse two sp functions for Mn, 6-311G(d) for O, N, and Cl, the relativistic effective-core potential and (111/111/1) for I, and 6-31G for C and H.

■ ASSOCIATED CONTENT

Ⓢ Supporting Information

Figure S1−S17. This material is available free of charge via the Internet at http://pubs.acs.org.

■ AUTHOR INFORMATION

Corresponding Author

*E-mail: hiro@ims.ac.jp.

Notes

The authors declare no competing financial interest.

■ ACKNOWLEDGMENTS

We thank Professor Masahito Ochiai for helpful comments on the preparation of iodosylarenes. This work was supported by grants from Japan Society for the Promotion of Science (Grant-in-Aid for Scientific Research, Grant Nos. 22350030 and 23550086).

■ REFERENCES

(1) *Biomimetic Oxidations Catalyzed by Transition Metal Complexes*; Imperial College Press: London, 2000.

(2) Zhdankin, V. V.; Stang, P. J. *Chem. Rev.* **2008**, *108*, 5299−5358.

(3) (a) Smegal, J. A.; Hill, C. L. *J. Am. Chem. Soc.* **1983**, *105*, 3515−3521. (b) Smegal, J. A.; Schardt, B. C.; Hill, C. L. *J. Am. Chem. Soc.* **1983**, *105*, 3510−3515.

(4) (a) Nam, W.; Choi, S. K.; Lim, M. H.; Rohde, J. U.; Kim, I.; Kim, J.; Kim, C.; Que, L., Jr. *Angew. Chem., Int. Ed.* **2003**, *42*, 109−111. (b) Song, W. J.; Sun, Y. J.; Choi, S. K.; Nam, W. *Chem.—Eur. J.* **2005**, *12*, 130−137.

(5) Guo, M.; Dong, H.; Li, J.; Cheng, B.; Huang, Y. Q.; Feng, Y. Q.; Lei, A. *Nat. Commun.* **2012**, *3*, 1190.

(6) Yang, Y. H.; Diederich, F.; Valentine, J. S. *J. Am. Chem. Soc.* **1990**, *112*, 7826−7828.

(7) (a) Ochiai, M.; Miyamoto, K.; Shiro, M.; Ozawa, T.; Yamaguchi, K. *J. Am. Chem. Soc.* **2003**, *125*, 13006−13007. (b) Ochiai, M.; Miyamoto, K.; Yokota, Y.; Suefuji, T.; Shiro, M. *Angew. Chem., Int. Ed.* **2004**, *44*, 75−78.

(8) (a) Bryliakov, K. P.; Talsi, E. P. *Angew. Chem., Int. Ed.* **2004**, *43*, 5228−5230. (b) Bryliakov, K. P.; Talsi, E. P. *Chem.—Eur. J.* **2007**, *13*, 8045−8050.

(9) (a) Wang, S. H.; Mandimutsira, B. S.; Todd, R.; Ramdhanie, B.; Fox, J. P.; Goldberg, D. P. *J. Am. Chem. Soc.* **2004**, *126*, 18−19. (b) Leeladee, P.; Goldberg, D. P. *Inorg. Chem.* **2010**, *49*, 3083−3085.

(10) (a) Song, W. J.; Seo, M. S.; George, S. D.; Ohta, T.; Song, R.; Kang, M. J.; Tosha, T.; Kitagawa, T.; Solomon, E. I.; Nam, W. *J. Am. Chem. Soc.* **2007**, *129*, 1268−1277. (b) Ottenbacher, R. V.; Bryliakov, K. P.; Talsi, E. P. *Inorg. Chem.* **2010**, *49*, 8620−8628.

(11) (a) Adam, W.; Roschmann, K. J.; Saha-Möller, C. R. *Eur. J. Org. Chem.* **2000**, *2000*, 3519−3521. (b) Adam, W.; Roschmann, K. J.; Saha-Möller, C. R.; Seebach, D. *J. Am. Chem. Soc.* **2002**, *124*, 5068−5073.

(12) (a) Collman, J. P.; Chien, A. S.; Eberspacher, T. A.; Brauman, J. I. *J. Am. Chem. Soc.* **2000**, *122*, 11098−11100. (b) Collman, J. P.; Zeng, L.; Decréau, R. A. *Chem. Commun.* **2003**, 2974. (c) Collman, J. P.; Zeng, L.; Brauman, J. I. *Inorg. Chem.* **2004**, *43*, 2672−2679.

(13) Linde, C.; Koliai, N.; Norrby, P. O.; Akermark, B. *Chem.—Eur. J.* **2002**, *8*, 2568−2573.

(14) Lennartson, A.; McKenzie, C. J. *Angew. Chem., Int. Ed.* **2012**, *51*, 6767−6770.

(15) Wang, C.; Kurahashi, T.; Fujii, H. *Angew. Chem., Int. Ed.* **2012**, *51*, 7809−7811.

(16) Jacobsen, E. N.; Zhang, W.; Muci, A. R.; Ecker, J. R.; Deng, L. *J. Am. Chem. Soc.* **1991**, *113*, 7063−7064.

(17) McGarrigle, E. M.; Gilheany, D. G. *Chem. Rev.* **2005**, *105*, 1563−1602.

(18) (a) Kurahashi, T.; Fujii, H. *Inorg. Chem.* **2008**, *47*, 7556−7567. (b) Kurahashi, T.; Hada, M.; Fujii, H. *J. Am. Chem. Soc.* **2009**, *131*, 12394−12405.

(19) Nam, W. W.; Valentine, J. S. *J. Am. Chem. Soc.* **1993**, *115*, 1772−1778.

(20) Izutsu, K. *Acid−Base Dissociation Constants in Dipolar Aprotic Solvents*; Blackwell Scientific Publications: Hoboken, NJ, 1990.

(21) Palucki, M.; Pospisil, P. J.; Zhang, W.; Jacobsen, E. N. *J. Am. Chem. Soc.* **1994**, *116*, 9333−9334.

(22) Park, S. E.; Song, W. J.; Ryu, Y. O.; Lim, M. H.; Song, R.; Kim, K. M.; Nam, W. *J Inorg Biochem* **2005**, *99*, 424−431.

(23) Stoll, S.; Schweiger, A. *J. Magn. Reson.* **2006**, *178*, 42−55.

(24) McGown, A. J.; Kerber, W. D.; Fujii, H.; Goldberg, D. P. *J. Am. Chem. Soc.* **2009**, *131*, 8040−8048.

(25) Kurahashi, T.; Fujii, H. *J. Am. Chem. Soc.* **2011**, *133*, 8307−8316.